Structural Investigation of Crystalline and Solution Phases in *N*,*N*,*N*′,*N*′-Tetramethylethylenediamine (TMEDA) with Lithium Triflate ($LiCF_3SO_3$) and Sodium Triflate ($NaCF_3SO_3$)

Rebecca A. Sanders, Roger Frech,* and Masood A. Khan

Department of Chemistry and Biochemistry, University of Oklahoma, Norman, Oklahoma 73019

Received: November 12, 2002; In Final Form: May 9, 2003

Linear poly(*N*-methylethylenimine) (LPMEI), a methylated derivative of linear poly(ethylenimine) (LPEI), shows potential as a polymer electrolyte host. The interactions of LPMEI with lithium and sodium cations are modeled by solutions of *N*,*N*,*N*′,*N*′-tetramethylethylenediamine, TMEDA, containing either dissolved lithium triflate (LiTf) or sodium triflate (NaTf). During these studies, crystalline compounds were discovered and characterized by X-ray diffraction, differential scanning calorimetry, and Fourier transform infrared spectroscopy (FT-IR). The TMEDA:LiTf crystallizes as dimers in an orthorhombic unit cell in the *Pccn* space group; however, the TMEDA:NaTf crystallizes as tetramers in a triclinic unit cell in the $P\bar{1}$ space group. A spectroscopic comparison of TMEDA, TMEDA:LiTf crystal, TMEDA:NaTf crystal, and their corresponding salt solutions over a composition range of 5:1 to 20:1 (nitrogen:cation, molar ratio) is carried out using FT-IR and Raman spectroscopy. The triple cation species $[Li_2Tf]^+$ is the dominant species in the TMEDA:LiTf solution and exclusively present in the crystal. However, the dominant species in the TMEDA:NaTf samples is the aggregate $[Na_3Tf]^{2+}$. The N−C−C−N dihedral angle, which appears to be a mixture of gauche minus and trans in both LiTf and NaTf solutions, changes to gauche minus upon crystallization. Finally, the vibrations of individual TMEDA molecules appear to be completely decoupled in the TMEDA:LiTf crystal, although each dimeric unit contains two TMEDA molecules.

1. Introduction

Polymer electrolytes offer a number of advantages for lithium rechargeable battery technology including high energy density, processibility, low environmental impact, and enhanced consumer safety.[1] The most widely studied polymer electrolyte is poly(ethylene oxide), PEO, complexed with various salts such as $LiCF_3SO_3$, $LiN(CF_3SO_2)_2$, $LiSbF_6$, $LiBF_4$, and $LiClO_4$. The mechanism of ionic transport in these systems is not well understood, especially at the molecular level. However, it is known that cation−anion interactions[2] and cation−polymer interactions[3] play critical roles in ion transport. Both cation−anion and cation−polymer interactions presumably affect the ionic mobilities; in addition, the former are expected to significantly affect the number of effective charge carriers. Cation−anion interactions lead to the formation of associated ionic species, while cation−polymer interactions are manifested in changes of the polymer backbone conformation. Thus local structures (ionically associated species and local backbone conformation) may be used to directly study the nature of those important interactions and provide essential insight needed to understand the mechanism of ionic transport.[4] Since polymer electrolytes are very complex structures, model compounds can provide crucial information about local structures in polymer electrolytes. Some of the compounds studied as models for PEO-based electrolytes include the dimethyl ethers of ethylene oxides or glymes, i.e., $CH_3(OCH_2CH_2)_nOCH_3$ with $n = 1-4$, complexed with various salts.

Glymes with dissolved salts are useful models of structure and dynamics in high molecular weight PEO−salt systems. In several cases, studies have shown that the conformational changes in the glyme−salt systems are strikingly similar to conformational changes in PEO complexed with the corresponding salt.[5,6] Further, polymers have been developed with ethylene oxide side chains as polymer electrolyte hosts; most notable among these is the family of polyphosphazenes with oligoethyleneoxy side groups.[7] Finally, computational studies have been performed on glyme−salt systems to gain insight into the nature of the ion transport mechanism in high molecular weight PEO−salt complexes.[8,9]

Linear poly(ethylenimine) or LPEI is a synthetically versatile polymer host compared to PEO, in that various groups can be attached to the backbone nitrogen atom. Pure LPEI has highly crystalline domains, therefore it exhibits poor conductivity. By adding various side chains (e.g., $-CH_3$) to LPEI, the crystallinity is decreased. Linear poly(*N*-methylethylenimine), LPMEI, is a methyl-substituted derivative of LPEI. LPMEI is completely amorphous at room temperature unlike LPEI, which melts at 58 °C.[10−12] To achieve a better understanding of LPMEI, *N*,*N*,*N*′,*N*′- tetramethylethylenediamine (TMEDA) is used as a model compound for LPMEI. While studying solutions of TMEDA with $LiCF_3SO_3$ (LiTf) and $NaCF_3SO_3$ (NaTf) in TMEDA, crystalline compounds were discovered. This paper describes the characterization of the crystalline and amorphous phases in TMEDA:LiTf and TMEDA:NaTf systems using X-ray diffraction, Fourier transform infrared spectroscopy (FT-IR), Raman spectroscopy, and differential scanning calorimetry (DSC). Structural information obtained from the TMEDA:LiTf and TMEDA:NaTf crystals provides a better understanding of the local environment of TMEDA and the triflate anion in TMEDA:LiTf and TMEDA:NaTf solutions.

* Corresponding author. Telephone: 1- 405-325-3831. Fax: 1- 405- 325-6111. E-mail: rfrech@ou.edu.

10.1021/jp022418k CCC: $25.00
Published on Web 07/23/2003

2. Experimental Section

2.1. Sample Preparation. *N*,*N*,*N*′,*N*′- Tetramethylethylenediamine (TMEDA), LiTf, and NaTf were obtained from Aldrich. TMEDA was distilled over sodium metal. LiTf and NaTf were heated under vacuum at 120 °C for 48 h. The chemicals were stored and used in a dry nitrogen glovebox (VAC, ≤1 ppm H_2O) at room temperature. To prepare the solutions, LiTf was dissolved into TMEDA at various concentrations and stirred for at least 48 h. Similar sample preparation was used for the NaTf samples except the samples were stirred only for 4 h. The compositions of the solutions are reported as a nitrogen to cation molar ratio (N:M, M = Li, Na). At higher triflate compositions, the solutions contained both a liquid and a gel-like phase that formed within 24 h of preparing the sample. Eventually, all the samples become phase-separated. Several months later, a fine-grained, gritty textured material had formed at the gel−liquid interface and on the glass surface just above the sample. After about 6 months, the entire sample was composed of crystals with only a small amount of residual solvent in the vial. The crystals were allowed to completely dry in a nitrogen atmosphere. The formation of crystals was evident in all of the TMEDA:LiTf and TMEDA:NaTf samples prepared.

2.2. X-ray. Single crystals for X-ray analysis were grown and isolated from a 38:1 TMEDA:LiTf solution and a 20:1 TMEDA:NaTf solution. X-ray data were collected at 173(2) K on a Bruker P4 diffractometer using Mo Kα radiation (λ = 0.710 73 Å). The data were corrected for Lorentz and polarization effects; an absorption correction was not applied since it was judged to be insignificant. The structure was solved by the direct method using the SHELXTL system and refined by full-matrix least squares on F^2 using all reflections. All non-hydrogen atoms were refined anisotropically, and all hydrogen atoms were included with idealized parameters.

For the TMEDA:LiTf crystal, the final $R1 = 0.068$ is based on 1541 "observed reflections" [$I > 2\sigma(I)$], and $wR^2 = 0.201$ is based on all reflections (2406 unique data). For the TMEDA:NaTf crystal, the final $R1 = 0.056$ is based on 6277 "observed reflections" [$I > 2\sigma(I)$], and $wR^2 = 0.153$ is based on all reflections (9715 unique data). In the TMEDA:NaTf crystal, some parts of the TMEDA are disordered as evident by the large thermal parameters of these atoms. In addition, the positions of the C17 and C18 atoms are not well defined; therefore, these atoms were resolved in two components with a 50% occupancy for each component.

2.3. Differential Scanning Calorimetry. A single crystal weighing approximately 3.5 mg was sealed in a 40-μL aluminum pan. For both crystals, DSC data were collected with a Mettler DSC 820 calorimeter with Star^e software (v.6.10) under dry nitrogen purge. The TMEDA:LiTf crystal data were collected during two heating and cooling cycles between 0 and 250 °C at a heating and cooling rate of 5 deg/min. However, the TMEDA:NaTf crystals were cycled between 0 and 300 °C at rate of 5 deg/min.

2.4. FT-IR and Raman Spectroscopy. For FT-IR measurements, the TMEDA, TMEDA:LiTf solutions, and TMEDA:NaTf solutions were placed between zinc selenide windows in a sealed sample holder. Finely ground crystals were prepared as KBr pellets. FT-IR data were recorded on a Bruker IFS66V with a KBr beam splitter over a range of 500−4000 cm^{-1} (1-cm^{-1} resolution). The spectra of the solutions were measured under a dry air purge; the crystal data were collected under vacuum (8 mbar). For the Raman measurements, the TMEDA and TMEDA:LiTf solutions were placed in a solution well and covered with a glass cover plate; the single crystal was sealed into a quartz cuvette in the glovebox. Raman data were recorded with a Jobin-Yvon T64000 system in the triple subtractive mode with a CCD detector using the 514.5 nm line of an argon laser for excitation. All Raman data were collected in a 180° scattering geometry at a laser power of 300 mW measured at the laser head.

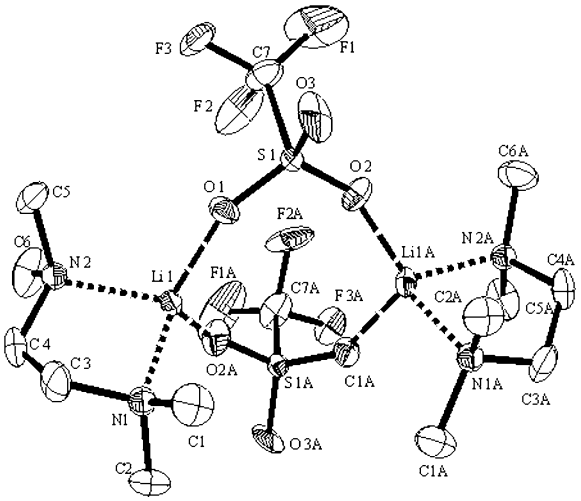

Figure 1. Dimer of the TMEDA:LiTf crystal showing the 4-fold coordination of the lithium atom.

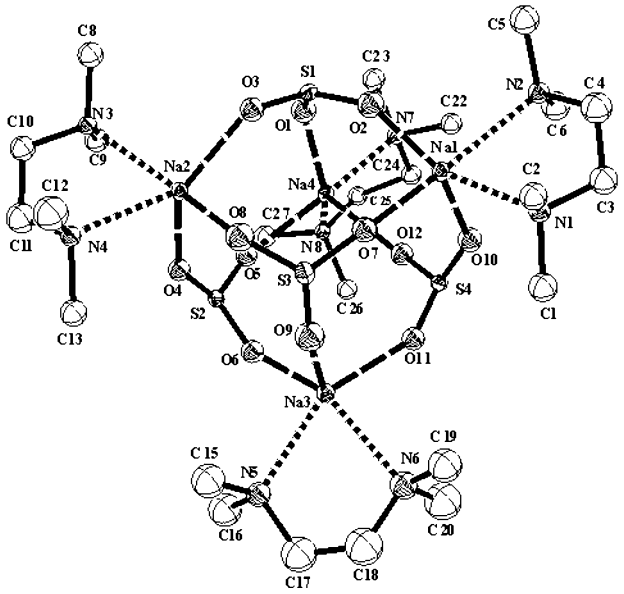

Figure 2. Tetramer of the TMEDA:NaTf crystal. The CF_3 groups of the triflate ions are not shown for clarity of the figure.

3. Results and Discussion

3.1. Crystal Structure. The TMEDA:LiTf crystal forms an orthorhombic unit cell in the *Pccn* space group with $Z = 8$; the structure consists of independent $(TMEDA:LiTf)_2$ dimers (Figure 1). Each lithium ion is coordinated by two nitrogen atoms and two triflate oxygen atoms, one from each of the two triflate ions in the dimer. The TMEDA:NaTf crystal forms a triclinic unit cell in the $P\bar{1}$ space group, which contains two tetramers $(TMEDA:NaTf)_4$ as illustrated in Figure 2. The sodium ion is coordinated to three triflate oxygen atoms and two nitrogen atoms. Structural data are summarized in Table 1; selected bond lengths and angles for the TMEDA:LiTf and TMEDA:NaTf crystals are listed in Tables 2 and 3.

The dimeric TMEDA:LiTf crystal structure is similar to the dimeric crystal structure of diglyme $[CH_3(OCH_2CH_2)_2OCH_3]$:

TABLE 1: Structural Data of the TMEDA:LiTf and TMEDA:NaTf Crystals

parameters	TMEDA LiTf	TMEDA NaTf
crystal system	orthorhombic	triclinic
space group	Pccn	$P\bar{1}$
temperature	173(2) K	173(2) K
A, Å	12.272(3)	10.6695(14)
B, Å	13.544(3)	12.5383(16)
C, Å	16.425(4)	22.392(3)
α	90°	92.054(9)°
β	90°	100.104(9)°
γ	90°	107.611(9)°
volume, Å^3	2730.1(12)	2798.3(7)
Z	8	2
density, mg/m^3	1.325	1.369
*R*1	0.068	0.056
crystal size, mm^3	0.54 0.52 0.24	0.38 0.36 0.32

TABLE 2: Selected Bond Lengths (Å) and Angles (deg) for the TMEDA:LiTf and TMEDA:NaTf Crystals

bond	X = Li	X = Na	bond	X = Li	X = Na
X−N	2.077(5)	2.502(2)	X−O	1.805(6)	2.269(2)
	2.066(5)	2.521(2)		1.836(6)[a]	2.283(2)
		2.472(2)		1.956(7)[a]	2.2830(18)
		2.519(2)		1.987(6)	2.276(2)
		2.489(3)			2.2779(19)
		2.523(3)			2.2864(19)
		2.495(2)			2.261(2)
		2.5101(18)			2.303(2)
					2.3160(19)
					2.270(2)
					2.2722(19)
					2.310(2)
bond sequence					
N−X−N	89.18(18)	73.19(7)			
		72.67(7)			
		71.29(9)			
		72.22(7)			

[a] The symmetry transformation ($-x + 1/2, -y + 1/2, z$) used to generate equivalent atoms.

LiTf or G2:LiTf, although in the G2:LiTf crystal the lithium atom is coordinated to three oxygen atoms of G2 and two triflate oxygen atoms.[5] An additional structural comparison can also be made with monoglyme [$CH_3(OCH_2CH_2)OCH_3$]:LiTf, G1:LiTf, where the lithium ion is four-coordinate in the crystalline compound.[13] Both TMEDA and G1 have two heteroatoms that provide coordinating sites for the lithium ion. However, TMEDA has two methyl groups attached to the nitrogen atom, whereas G1 has only one methyl group coordinated to the ether oxygen. Therefore, the greater steric hindrance in TMEDA plays a role in its coordination chemistry. For example, in the G1:LiTf crystal each G1 molecule is coordinated to two different lithium atoms.[13] Further, the lithium ion in the G1:LiTf crystal is also coordinated to three different triflate oxygen atoms, unlike the lithium ion−triflate ion coordination in the TMEDA:LiTf crystal.[13]

The conformational structures of the TMEDA oligomers can be characterized in terms of the C−N−C−C and N−C−C−N dihedral angles (gauche, g, 60 ± 30°; gauche minus, $\bar{g}$, −60 ± 30°; s, 120 ± 30°; s minus, $\bar{s}$, −120 ± 30° trans, t, ±180 ± 30°). An individual TMEDA molecule can occur in four different conformations because of the two methyl groups attached to each nitrogen atom. However, the N−C−C−N dihedral angle is of most interest because it is directly affected by the coordination of the cation to the nitrogen atoms. In the TMEDA:LiTf crystal (Table 3), the N−C−C−N dihedral angle (−54.0°) leads to conformations x$\bar{g}$x′ where x, x′ = t or $\bar{g}$. However, the TMEDA:NaTf crystal has four different N−C−C−N dihedral angles (−53.1°, −60.3°, 55.4°, 42.3°), which leads to two TMEDA molecules with x$\bar{g}$x′ (x, x′ = t or $\bar{g}$), one with x_1gx_1' (x_1, x_1' = t or g), and one with either x_2gx_2' (x_2, x_2' = $\bar{s}$ or s) or $x_3\bar{g}x_3'$ (x_3, x_3' = $\bar{g}$ or t) conformations. There are two possible conformations about the C17 and C18 bond because these atoms are disordered.

TABLE 3: Dihedral Angles of TMEDA:LiTf and TMEDA:NaTf Crystals with the Corresponding Conformations

bond sequence	dihedral angle, deg	conformation
	TMEDA:NaTf	
C−N1−C−C	154.6(3)	t
C−N1−C−C	−84.1(3)	$\bar{g}$
N1−C−C−N2	−53.1(4)	$\bar{g}$
C−C−N2−C	−85.8(4)	$\bar{g}$
C−C−N2−C	156.0(3)	t
C−N3−C−C	−154.0(2)	t
C−N3−C−C	85.7(3)	g
N3−C−C−N4	55.4(3)	g
C−C−N4−C	74.4(3)	g
C−C−N4−C	−164.9(2)	t
C−N5−C−C	−145.0(6), 158.2(4)	$\bar{s}$, t
C−N5−C−C	95.9(7), −83.1(5)	s, $\bar{g}$
N5−C−C−N6	42.3(8), −65.4(6)	g, $\bar{g}$
C−C−N6−C	105.2(5), −69.9(7)	s, $\bar{g}$
C−C−N6−C	−138.1(5), 166.8(5)	$\bar{s}$, t
C−N7−C−C	167.2(2)	t
C−N7−C−C	−72.3(3)	$\bar{g}$
N7−C−C−N8	−60.3(3)	$\bar{g}$
C−C−N8−C	−77.0(3)	$\bar{g}$
C−C−N8−C	162.3(2)	t
	TMEDA:LiTf	
C1−N−C3−C4	158.0(3)	t
C2−N−C3−C4	−80.6(4)	$\bar{g}$
N−C3−C4−N	−54.0(5)	$\bar{g}$
C3−C4−N−C5	−81.2(4)	$\bar{g}$
C3−C4−N−C6	158.3(4)	t

The TMEDA conformations in the TMEDA:LiTf crystal (x$\bar{g}$x′) differ from those in the crystals of G1:LiTf (ttt) and G2:LiTf (tgt - t$\bar{g}$t). The major difference is in the x−C−C−x dihedral angles (x = N, O), which are gauche minus in TMEDA:LiTf, trans in G1:LiTf, and gauche/gauche minus in G2:LiTf.[5,13] These differences are mainly due to packing requirements originating in the different molecular structures of the organic constituents.

The Li−N bond length (∼2.08 Å) in the TMEDA:LiTf crystal is 0.42 Å shorter than the Na−N bond length (∼2.50 Å) in the TMEDA:NaTf crystal (Table 2). In addition, the Li−O bond length (∼1.90 Å) is 0.38 Å shorter than the Na−O bond length (∼2.28 Å). These differences are greater than the differences in their ionic radii, therefore suggesting the lithium ion is more strongly coordinated to both the nitrogen and oxygen atom compared to the sodium ion. There is also a 17° difference between the N−Li−N (∼89°) and N−Na−N (∼72°) bond angles, which correlates with the differences in the cation−nitrogen bond lengths. However, changing the cation does not significantly affect the F−C−F bond angles or the C−C and C−N bond distances (data not shown).

The Li−N bond length (∼2.08 Å) in the TMEDA:LiTf crystal is slightly longer than the Li−O (ether oxygen) bond length in G1:LiTf (1.93 Å) and similar to that in the G2:LiTf crystals (2.10 Å).[5] In addition, the Li−O (triflate oxygen) bond distances in the TMEDA:LiTf crystal (1.81−1.99 Å) have a greater spread of values compared to G1:LiTf (1.93−1.94 Å) and G2:LiTf (1.94−1.97 Å).[5,13] The Li−O−S angles in the TMEDA:LiTf crystal (136.9−168.0°) are very similar to the Li−O−S (triflate oxygen) bond angles in the G2:LiTf crystal (144−161°).[14]

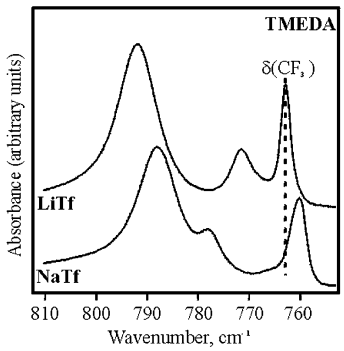

Figure 3. FT-IR spectra of crystalline TMEDA:LiTf and TMEDA:NaTf in the 750−810 cm^{-1} region.

3.2. Thermal Analysis. Differential scanning calorimetry (DSC) was used to characterize melting and recrystallization processes in the TMEDA:LiTf and TMEDA:NaTf crystals. In the DSC thermogram of the TMEDA:LiTf crystal (figure not shown), there is a endothermic sharp peak at 154 °C due to the melting of the crystalline compound. The onset of recrystallization occurs at 110 °C. In a second thermal analysis cycle, the melting and recrystallization temperatures decrease to 128 and 107 °C, respectively, indicating some degree of thermal hysteresis. However, the data may also be interpreted as incongruent melting/recrystallization. In addition, the melting peak becomes smaller and broader, indicating a loss of crystallinity of the sample. The TMEDA:LiTf crystal is more thermally stable compared to the G1:LiTf or the G2:LiTf crystals, which melt at −3 and 27 °C, respectively.[5,13]

The thermogram of the TMEDA:NaTf crystal (figure not shown) is different than the thermogram of the TMEDA:LiTf crystal. For instance, TMEDA:NaTf has four endothermic phase transitions occurring at 128, 193, 199, and 237 °C in the first heating cycle. Only the two transitions at 128 and 237 °C appear in the cooling cycles and are observed at 110 and 238 °C. During the second heating cycle these transitions occur at 118 and 238 °C. In addition, the peak at ∼110 °C becomes broader and smaller, indicating a decrease in the crystallinity of the sample. However, the phase transition at 237 °C is completely reversible, with no hysteresis within experimental error. The melting temperature of the TMEDA:NaTf crystal is higher than that of the TMEDA:LiTf crystal, partly because the crystal consists of a much larger network structure.

3.3. Vibrational Spectroscopy. Knowledge of the TMEDA:LiTf and TMEDA:NaTf crystal structures provides unambiguous information about the local structures in the crystals. In turn, this knowledge can result in critical insight into local structures in TMEDA:LiTf and TMEDA:NaTf solutions through comparative spectroscopic studies of both crystalline and solution phases. This is accomplished by identifying the spectral signatures of local structures in the TMEDA:LiTf and TMEDA:NaTf crystals, with particular attention to the bands from 770 to 1000 cm^{-1}. The frequencies and intensities of bands in this region are sensitive to conformational changes in the TMEDA backbone. Bands in this region have also been shown to provide information about backbone conformation in ethylene oxide-based systems.[15] Figure 3 shows that there are some differences between the crystalline TMEDA:LiTf and TMEDA:NaTf spectra in this conformation-sensitive region. The bands at 772 (TMEDA:LiTf) and 778 cm^{-1} (TMEDA:NaTf) are predominately due to CH_2 rocking motion.[15] In addition, the TMEDA band at 792 cm^{-1} in the TMEDA:LiTf crystal spectrum is 4 cm^{-1} higher than in the TMEDA:NaTf crystal spectrum. It is important to note that in the TMEDA:NaTf crystal, the 788-cm^{-1} band is attributed primarily to a predominant CH_2 twisting motion.[16] However, the 792 cm^{-1} band in the TMEDA:LiTf crystal is due to a mixed mode of C−N stretching, CH_2 twisting, and CH_2 wagging motions.[15]

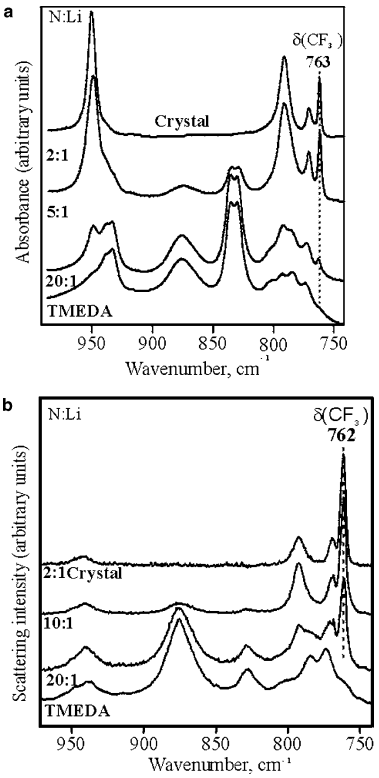

Figure 4. (a) FT-IR spectra and (b) Raman spectra of TMEDA with varying concentrations of LiTf in the $\delta(CF_3)$ and conformation regions.

From parallel studies of crystalline TMEDA:LiTf, TMEDA, and solutions of LiTf in TMEDA, information about the conformational changes of TMEDA resulting from lithium ion coordination in TMEDA:LiTf solutions can be inferred. For instance, in Figure 4a, the FT-IR bands in the predominantly C−N stretching region at 830, 835, and 876 cm^{-1} diminish in intensity with increasing LiTf concentration and completely disappear in the spectrum of the TMEDA:LiTf crystal.[16] Computational studies of TMEDA in the gas phase attribute these bands of TMEDA to a trans N−C−C−N dihedral angle.[16] However, the bands in the 700−800 cm^{-1} and 900−1000 cm^{-1} regions are due to a TMEDA molecule with a gauche minus N−C−C−N dihedral angle.[16] Therefore, the N−C−C−N dihedral angle, which is a mixture of gauche and trans in the TMEDA:LiTf solutions, appears to change to gauche minus upon crystallization. This interesting phenomenon is also observed in the Raman spectra (Figure 4b) and TMEDA:NaTf spectra (Figure 5). Striking differences between solution spectra and crystalline spectra reflecting dramatic conformational changes upon crystallization were also observed in the G1:LiTf system.[13] However, in that system the O−C−C−O dihedral angle of G1 changes from gauche in solution to trans upon crystallization.[13]

Bands in the range 770−810 cm^{-1} and 930−940 cm^{-1} are also affected by the conformational changes during crystallization of the TMEDA:LiTf and TMEDA:NaTf compounds. In TMEDA (Figure 4a), there are at least four bands in the 770−810 cm^{-1} region. A computational analysis established that the TMEDA bands in this region are a complex mixture of C−C and C−N stretching, CH_2 wagging, CH_2 twisting, and CH_2 rocking motions.[17] The bands at 772 and 792 cm^{-1} become more

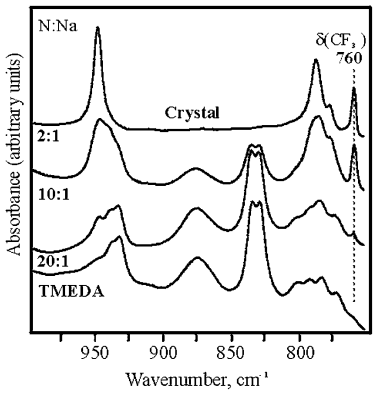

Figure 5. FT-IR spectra of TMEDA with varying concentrations of NaTf in the $\delta(CF_3)$ and conformation regions.

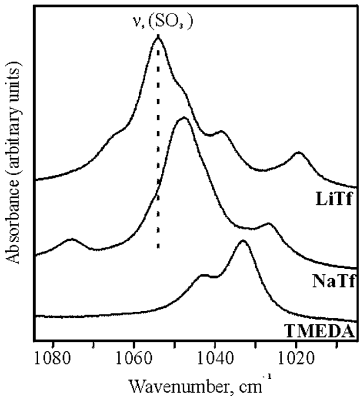

Figure 6. FT-IR spectra of TMEDA with varying LiTf and NaTf concentrations in the $\nu_s(SO_3)$ region.

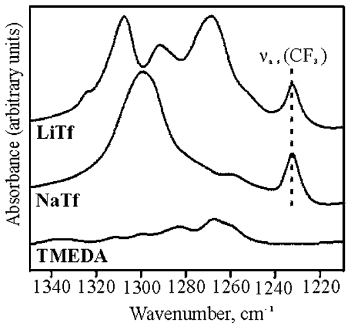

Figure 7. FT-IR spectra of the TMEDA and TMEDA crystals with NaTf and LiTf the $\nu_{as}(SO_3)$ and $\nu_{as}(CF_3)$ regions.

prominent with increasing LiTf concentrations until, in the crystal, they are the dominant TMEDA bands in this region. Similar results are seen in the TMEDA:NaTf samples (Figure 5) where the two prominent bands in the crystal are at 778 and 788 cm^{-1}.

The nature of the vibrational modes of the TMEDA bands in this region ($\sim$780 cm^{-1}) changes upon addition of salt. When NaTf is added to TMEDA, the TMEDA modes change from C−C and C−N stretching, CH_2 wagging, and CH_2 twisting motions to a predominately CH_2 twisting motion.[17] However, when LiTf is added, the TMEDA modes in this region involve primarily C−N stretching, CH_2 wagging, and CH_2 twisting motions.[17]

The change in TMEDA conformation has a more dramatic effect on the 930−940 cm^{-1} region, which is comprised mostly of CH_2 rocking, C−C stretching, and CH_3 wagging motions.[17] Even in a 20:1 solution composition of TMEDA:LiTf or TMEDA:NaTf, a few bands suggest the early formation of local structures similar to those in the crystal. In Figure 4a, the band at 949 cm^{-1} increases in intensity and shifts to a higher frequency (951 cm^{-1}) with increasing LiTf concentration. Similar behavior is seen in the Raman data shown in Figure 4b. However, when NaTf is added to TMEDA, the 949-cm^{-1} band does not shift upon crystallization within experimental error (1 cm^{-1}). In TMEDA:LiTf, this band (949 cm^{-1}) consist primarily of CH_2 rocking motion; however, in TMEDA:NaTf, this band (948 cm^{-1}) is due to both CH_2 rocking and CH_2 twisting motions.[17]

The CF_3 symmetric deformation, $\delta(CF_3)$, region contains distinct bands due to different ionically associated species: "free" ions at 752−753 cm^{-1}, contact ion pairs [MTf] (M = cation) at 756−758 cm^{-1}, and the aggregate species $[M_2Tf]^+$ or $[M_3Tf]^{2+}$ at 761−763 cm^{-1}.[18−21] Therefore, a spectral study of this region can provide additional local structural information about the coordination of the triflate ion by the lithium and sodium ion(s). The spectra−structure correlations of the triflate ion species quoted above have been determined in ethylene oxide-based systems. Therefore, it is necessary to either develop a similar set of correlations in TMEDA or confirm that the ethylene oxide-based correlations may be used in TMEDA systems. In the TMEDA:LiTf crystal, the $\delta(CF_3)$ band is measured at 763 cm^{-1} (IR) and 762 cm^{-1} (Raman), Figure 4a,b. Based on the crystal structure, this frequency is associated with an aggregate species where one triflate ion is coordinated to two lithium ions, $[Li_2Tf]^+$. The $[Li_2Tf]^+$ aggregate is the dominant species in all TMEDA:LiTf solutions. The frequency of $[Li_2Tf]^+$ in the TMEDA:LiTf crystal agrees well with its frequency in the G2:LiTf crystal, where it is observed at 763 cm^{-1} (Raman).[5]

In the TMEDA:NaTf crystal, the $\delta(CF_3)$ band is at 760 cm^{-1}, which can be unambiguously associated with the aggregate species $[Na_3Tf]^{2+}$. This species dominates even in the solution phase. As illustrated in Figure 3, there is a 3 cm^{-1} difference in the $\delta(CF_3)$ band maximum between TMEDA:LiTf and TMEDA:NaTf crystal spectra. Even though the TMEDA:NaTf forms a higher order aggregate species than TMEDA:LiTf, this species has a slightly lower frequency because the sodium atom is not as strongly coordinated to the triflate ion. In addition, the $\delta(CF_3)$ band in the TMEDA:NaTf spectra has a larger bandwidth than in the TMEDA:LiTf spectra.

The frequency of the SO_3 symmetric stretch, $\nu_s(SO_3)$, is also affected by the coordination of the triflate ion with the cation. Raman-active bands at 1032−1033 cm^{-1}, 1037−1042 cm^{-1}, and 1044−1056 cm^{-1} correspond to "free" ions, contact ion pairs, and aggregate species, respectively, in ethylene oxide-based systems.[18−21] In Figure 6, the $\nu_s(SO_3)$ band in the infrared spectra appears at 1054 cm^{-1} (TMEDA:LiTf crystal) and 1048 cm^{-1} (TMEDA:NaTf crystal). This frequency difference in the $\nu_s(SO_3)$ band is again due to the relatively weaker coordination of the sodium atom with the triflate ion oxygen atoms. The latter frequency is the same, within experimental error, as in the ethylene oxide systems. The Raman frequency of the $\nu_s(SO_3)$ mode in the TMEDA:LiTf crystal (1051 cm^{-1}) is comparable to that in the G2:LiTf crystal (1053 cm^{-1}) because the triflate ion vibrates as a $[Li_2Tf]^+$ species in both crystals.[5] The $\nu_s(SO_3)$ frequency (Raman) is higher in the G1:LiTf crystal (1056 cm^{-1}) because there the triflate ion is coordinated to three lithium ions.[5,13]

The SO_3 asymmetric stretch, $\nu_{as}(SO_3)$, of the triflate ion is also affected by coordination to the cations, as illustrated in Figure 7. The apparent simplicity of the TMEDA:NaTf crystal spectrum in this region is deceptive. The 2-fold degeneracy of the $\nu_{as}(SO_3)$ mode in an isolated triflate ion is broken by the

potential energy environment in the crystal. Formally, each of the four triflate ions in the asymmetric unit yields two components resulting from the broken degeneracy, for a total of eight vibrational degrees of freedom. However, there are two tetrameric units in the unit cell, i.e., $Z = 2$. Therefore, there are a total of 16 vibrational degrees of freedom originating in the $\nu_{as}(SO_3)$ mode. These vibrational components are then correlated through intermolecular interactions, resulting in a vibrational multiplet structure that can be analyzed by standard group theoretical methods.[22] The irreducible representations of these modes under the $P\bar{1}$ unit cell group are given by

$$\Gamma(\nu_{as}(SO_3)) = 8A_g + 8A_u \quad (1)$$

This analysis predicts eight infrared-active $\nu_{as}(SO_3)$ vibrational modes. The data in Figure 7 show that the splitting in this mode induced by the interaction with the sodium ion and the subsequent coupling interaction of the eight triflate ions in the unit cell are not sufficient to resolve the individual modes predicted by eq 1. However, the breadth of the feature in Figure 7 probably originates in the overlap of these components.

There are also 16 degrees of vibrational freedom arising from $\nu_{as}(SO_3)$ in the TMEDA:LiTf crystal. A correlation field analysis shows that the $\nu_{as}(SO_3)$ modes can be classified according to the irreducible representations of the *Pccn* unit cell group as

$$\Gamma(\nu_{as}(SO_3)) = 2A_g + 2B_{1g} + 2B_{2g} + 2B_{3g} + 2A_u + 2B_{1u} + 2B_{2u} + 2B_{3u} \quad (2)$$

Because the sample was in the form of a microcrystalline powder, in principle all six infrared-active components ($2B_{1u} + 2B_{2u} + 2B_{3u}$) are observed in a transmission experiment. In the spectrum, prominent bands are observed at 1307 and 1268 cm^{-1}, with a smaller, asymmetric band at 1292 cm^{-1}. In addition, a very weak band occurs at 1324 cm^{-1}. Without an oriented single crystal and a complete set of polarized infrared reflection spectra, a detailed assignment of these four bands in terms of their symmetry species is not possible. In this region, the CF_3 asymmetric stretching mode occurs at 1230 cm^{-1} in both the TMEDA:LiTf and TMEDA:NaTf crystal spectra.

4. Conclusions

Single crystals of TMEDA:LiTf and TMEDA:NaTf have been isolated and characterized by X-ray diffraction, DSC, FT-IR, and Raman techniques. The TMEDA:LiTf crystal (dimer) is structurally different than the TMEDA:NaTf crystal (tetramer), where the lithium ion is four-coordinate and the sodium ion is five-coordinate.

Since the TMEDA:LiTf crystal structure is described by the *Pccn* (D_{2h}^{10}) space group, it has a center of symmetry. Therefore, modes should be either Raman active or infrared active, but none should be simultaneously Raman and infrared active except by coincidence. However, in the TMEDA:LiTf crystal, the majority of the vibrational bands are both IR and Raman active. This suggests that the two TMEDA molecules are vibrationally decoupled; i.e., the vibrations of each TMEDA molecule are sufficiently independent such that the role of the inversion center in coupling vibrations is negligible.

This work demonstrates that spectroscopic studies of the TMEDA:LiTf and TMEDA:NaTf crystals can provide insight into the local structures present in solutions of TMEDA:LiTf and TMEDA:NaTf. Specifically, local structures similar to those in the crystal are present in the TMEDA:LiTf and TMEDA:NaTf solutions, even at a 20:1 composition. In addition, there is evidence of conformational changes occurring in the solutions upon crystallization. A comparison of computational studies in the gas phase, X-ray analyses of the crystal structures, and vibrational measurements of crystalline and solution phases lead to the conclusion that conformation of TMEDA in the TMEDA:LiTf and TMEDA:NaTf solutions changes from a mixture of x$\bar{g}$x and xtx to x$\bar{g}$x upon crystallization of the TMEDA:LiTf and TMEDA:NaTf compounds. In addition, the ionic association in TMEDA:LiTf and TMEDA:NaTf solutions is similar to that in the TMEDA:LiTf and TMEDA:NaTf crystals, where the $[Li_2Tf]^+$ and $[Na_3Tf]^{2+}$ aggregate species are the primary ionic species present, even in a 20:1 composition.

The lithium ion is more strongly coordinated to both the nitrogen and oxygen atoms than is the sodium ion. Therefore, larger frequency shifts in similar bands and changes in the vibrational modes are observed when comparing TMEDA:LiTf to TMEDA:NaTf. Similar results are seen in the poly(ethylene oxide) systems where the lithium ion is more strongly coordinated to the ether oxygen atoms than is the sodium ion.

Finally there are some striking similarities between the TMEDA:LiTf crystal and several glyme:LiTf crystals. Both TMEDA:LiTf and G2:LiTf crystallize as discrete dimers comprised of two cations, two anions, and two solvent molecules. However, the lithium ion is 4-fold coordinated in the TMEDA:LiTf crystal and 5-fold coordinated in the G2:LiTf crystal. Upon crystallization, the solvent molecules in both TMEDA:LiTf and G1:LiTf undergo dramatic changes in conformation as shown by the values of the N−C−C−N and O−C−C−O dihedral angles, respectively.

Acknowledgment. This work was partially supported by funds from the National Science Foundation, Contract No. DMR-0072544. We appreciate the assistance of Scott Boesch in the ab initio calculations.

References and Notes

(1) Gauthier, M.; Bélanger, A.; Kapfer, B.; Vassort, G.; Armand, M. *Polymer Electrolyte Reviews Volume 2*; Elsevier: London, 1989.
(2) Papke, B. L.; Ratner, M. A.; Shriver, D. F. *J. Electrochem. Soc.* **1982**, *129*, 1434−1438.
(3) Armand, M. B.; Chabagno, J. M.; Duclot, M. J. *Sec. Int. Conf. on Solid Elect.* 1978, St. Andrews, Scotland.
(4) Bruce, P. G. *Faraday Discuss. Chem. Soc.* **1989**, *88*, 43−54.
(5) Rhodes, C. P.; Frech, R. *Macromolecules* **2001**, *34*, 2660−2666.
(6) Rhodes, C. P.; Khan, M.; Frech, R. *J. Phys. Chem. B* **2002**, *106*, 10 330−10 337.
(7) Allcock, H. R.; O'Connor, S. J. M.; Olmeijer, D. L.; Napierala, M. E.; Cameron, C. G. *Macromolecules* **1996**, *29*, 7544−7552.
(8) Borodin, O.; Smith, G. D. *Macromolecules* **1998**, *31*, 8396−8406.
(9) Sutjianto, A.; Curtiss, L. A. *J. Phys. Chem. A* **1998**, *102*, 968−974.
(10) Saegusa, T.; Ikeda, H.; Fujii, H. *Macromolecules* **1972**, *5*, 108.
(11) Chatani, Y.; Irie, T. *Polymer* **1988**, *29*, 2126−2129.
(12) Tanaka, R.; Ueoka, I.; Takaki, Y.; Kataoka, K.; Saito, S. *Macromolecules* **1983**, *16*, 849−853.
(13) Rhodes, C. P.; Khan, M.; Frech, R.; Ruf, M. *J. Phys. Chem.*, submitted for publication.
(14) Rhodes, C. *X-ray data of the diglyme: LiTf crystal*, unpublished results.
(15) Matsuura, H.; Fukuhara, K. *J. Polym. Sci. B* **1986**, *24*, 1383−1400.
(16) Boesch, S.; Wheeler, R. *Calculation of TMEDA: LiTf in the ttt conformation were performed using B3LYP, a hybrid Hartree−Fock density functional method, with a basis set of 6-31G(d)*, unpublished results.
(17) Boesch, S.; Wheeler, R. *Calculations (for vibrational mode assignments) of TMEDA, TMEDA:LiTf and TMEDA: NaTf were performed using B3LYP, a hybrid Hartree-Fock/density functional method, with a 6-31G(d) basis set*, unpublished results.
(18) Schantz, S.; Sandahl, J.; Borjesson, L.; Torell, L. M.; Stevens, J. R. *Solid State Ionics* **1988**, *28−30*, 1047−1053.
(19) Frech, R.; Huang, W. *Solid State Ionics* **1994**, *72*, 103−107.
(20) Huang, W.; Frech, R.; Wheeler, R. A. *J. Phys. Chem.* **1994**, *98*, 100−110.
(21) Frech, R.; Huang, W.; Dissanayake, M. A. K. L. *Mater. Res. Soc. Symp. Proc.* **1995**, *369*, 523−534.
(22) Fately, W. G.; Dollish, F. R.; McDevitt, N. T.; Bentley, F. F. *Infrared and Raman Selection Rules for Molecular and Lattice Vibrations: The Correlation Method;* Wiley-Interscience: New York, 1972.